Science

www.sciencemag.org
Science 3 July 2015:
Vol. 349 no. 6243 pp. 74-77
DOI: 10.1126/science.aaa9101

- REPORT

Cortical folding scales universally with surface area and thickness, not number of neurons

Bruno Mota[1], **Suzana Herculano-Houzel**[2,3,*]

+ Author Affiliations

*Corresponding author. E-mail: suzanahh@gmail.com

ABSTRACT | EDITOR'S SUMMARY

Larger brains tend to have more folded cortices, but what makes the cortex fold has remained unknown. We show that the degree of cortical folding scales uniformly across lissencephalic and gyrencephalic species, across individuals, and within individual cortices as a function of the product of cortical surface area and the

square root of cortical thickness. This relation is derived from the minimization of the effective free energy associated with cortical shape according to a simple physical model, based on known mechanisms of axonal elongation. This model also explains the scaling of the folding index of crumpled paper balls. We discuss the implications of this finding for the evolutionary and developmental origin of folding, including the newfound continuum between lissencephaly and gyrencephaly, and for pathologies such as human lissencephaly.

Related Resources

In *Science* Magazine

PERSPECTIVE
BRAIN EVOLUTION
Knowing when to fold them
Georg F. Striedter, Shyam Srinivasan
Science 3 July 2015: 31-32.

The expansion of the cerebral cortex, the most obvious feature of mammalian brain evolution, is generally accompanied by increasing degrees of folding of the cortical surface into sulci and gyri (*1*). Cortical folding has been considered a means of allowing numbers of neurons in the cerebral cortex to expand beyond what would be possible in a lissencephalic cortex, presumably as the cortical sheet expands laterally with a constant number of neurons beneath the surface (*2*, *3*). Although some models have shown cortical convolutions to form as a result of cortical growth (*4*, *5*), the mechanisms that drive gyrification remain to be determined, and the field still lacks a mechanistic and predictive, quantitative explanation for how the degree of cortical folding scales across species. Moreover, recent systematic analyses of cortical folding have made clear that gyrification actually scales differently across mammalian orders, across clades within an order, and across individuals as a function of increasing brain volume (*6*–*9*). These apparent discrepancies have led to the view that different mechanisms must regulate cortical folding at the evolutionary, species-specific, and ontogenetic levels (*7*).

We undertook a systematic analysis of the variation in cortical folding across a large sample of mammalian species in search of a universal, unifying relationship between cortical folding and morphological properties of the cerebral cortex. We examined two data sets: our own, which includes numbers of cortical neurons and cortical surface areas (*10*–*21*), and another consisting of published data on cortical surface area, thickness, brain volume, and folding index, but not numbers of cortical neurons (*1*, *22*–*24*) (table S1).

In the combined data set, there is a general correlation between total brain mass and the degree of cortical folding, and the two data sets overlap in their distribution (**Fig. 1A**, compare black and colored data points). However, the power function that relates the folding index of gyrencephalic species to brain mass has a fairly low r^2 and a 95% confidence interval that excludes many species (**Fig. 1A**). Striking and well-known outliers in this relationship are cetaceans (as a whole) and the manatee, but the capybara, the greater kudu, and humans also lie outside of the confidence interval (**Fig. 1A**). This indicates that cortical folding is not a homogeneous function of brain mass.

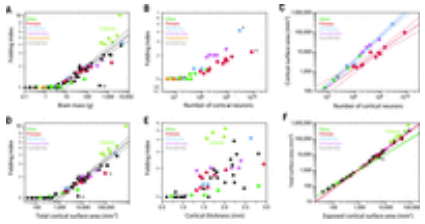

View larger version:

In this page In a new window

Download PowerPoint Slide for Teaching

Fig. 1. Scaling of cortical folding index and total cortical surface area.

Data points in black are taken from the literature; points in colors are from our own data set, except for cetaceans. (**A** to **E**) Folding index scales across all gyrencephalic species in the combined data sets as power functions of (A) brain mass, with exponent 0.221 ± 0.018 (r^2 = 0.751, P < 0.0001); (B) number of cortical neurons, with exponent 0.168 ± 0.032 (r^2 = 0.573, P < 0.0001; not plotted); (D) total cortical area, with exponent 0.257 ± 0.014 (r^2 = 0.872, P < 0.0001); and (E) average cortical thickness, with a nonsignificant exponent (r^2 = 0.054, P = 0.1430; not plotted). (C) Total cortical surface area of the cerebral cortex scales across primate species with an exponent of 0.911 ± 0.083 (r^2 = 0.938, P < 0.0001) and across nonprimate species with an exponent of 1.248 ± 0.037 (r^2 = 0.989, P < 0.0001). (**F**) Total cortical surface area varies across lissencephalic species as a linear function of the exposed surface area, but as a power function with an exponent of 1.242 ± 0.018 across noncetacean gyrencephalic species (r^2 = 0.992, P < 0.0001). Dashed lines are 95% confidence intervals for the fitted functions. Dashed lines are 95% confidence intervals for the fitted functions.

Although all cortical hemispheres with fewer than 30 million neurons are lissencephalic in our data set, and the correlation between folding index and number of neurons is significant across gyrencephalic species (Spearman correlation, ρ = 0.7741, P < 0.0001), the degree of gyrification is much larger in artiodactyls than in primates for similar numbers of cortical neurons (**Fig. 1B**). Additionally, the elephant cortex is about twice as folded as the human cortex, although the former has only about one-third the number of neurons found in the latter (**Fig. 1B**, “e” and “h”). The cortical surface area across species expands sublinearly with the number of cortical neurons in primates and supralinearly in other species (**Fig. 1C**). As a consequence, the average number of neurons per mm^2 of cortical surface is highly variable across species, ranging in our data set from 10,752 in the African elephant (*15*) to 138,606 in the squirrel monkey (*20*). Cortical expansion and folding are therefore neither a direct consequence of increasing numbers of neurons nor a requirement for increasing numbers of neurons in the cortex.

In comparison to the poor fit between folding index and total brain mass (**Fig. 1A**), a better fit is found for total surface area of the cerebral cortex in the two data sets (**Fig. 1D**). In this case, there is better overlap across afrotherians, glires, primates, and artiodactyls, although cetaceans, the manatee, and humans are still major outliers. Interestingly, all species with a cortical surface area below 400 mm^2 are lissencephalic in the two data sets. Similarly, all species with average cortical thickness below 1.2 mm are lissencephalic, but the folding index does not vary as a significant power function of cortical thickness across gyrencephalic species (**Fig. 1E**).

The folding index shows a sharp inflection between smooth and gyrated cortices, so it is unlikely that a universal model in terms of this variable alone could be derived. Because the folding index is the ratio of total surface area A_G to exposed surface area A_E, we next examined directly how A_E scales with A_G (**Fig. 1F**). In the combined data sets, for the species with small A_G (<400 mm^2) there is no folding, such that A_E equals A_G (**Fig. 1F**, green line). This linear relationship extends to the manatee cerebral cortex, even though its A_G is much larger than 1000 mm^2. In contrast, for all noncetacean gyrencephalic species, A_G increases with $A_E^{1.242\pm0.018}$ ($r^2 = 0.992$, $P < 0.0001$), significantly above linearity (**Fig. 1F**, red line), meaning that as total surface area increases, it becomes increasingly folded. Cetaceans fall above the 95% confidence interval of the function, which indicates that these cortices are more folded than similarly sized cortices in noncetaceans.

The finding that A_G scales as a power law of A_E means that gyrification is a property of a cortical surface that is self-similar down to a fundamental scale (the limit area between lissencephaly and gyrencephaly). This strongly suggests the existence of a single universal mechanism responsible for cortical folding (the alternative being some improbable multiscale fine-tuning) that over a range of scales generates self-similar, or fractal, surfaces.

Fractals can be characterized by the power-law scaling between intrinsic and extrinsic measures of an object's size, such as A_G and A_E. In this case, the fractal dimension d of the cortical surface is twice the value of the exponent relating A_G to A_E (given that A_E in turn scales with the square of the linear dimension of the cortex). Given that A_G scales with $A_E^{1.242\pm0.018}$ across noncetacean gyrencephalic brains, then $d = 2.484 \pm 0.036$. This value is remarkably close to the fractal dimension 2.5 of crumpled sheets of paper (*25*), which are fractal-like self-avoiding surfaces thin enough to fold under external compression while maintaining structural integrity.

Empirically, we conceive the fractal folding (or lack thereof) of the cortical surface as a consequence of the minimization of the effective free energy of a self-avoiding surface of average thickness T that bounds a volume composed of fibers connecting distal regions of said surface. Our model incorporates the known mechanics and organization of elongating axonal fibers (*26*, *27*), as described in the supplementary materials. It predicts that from a purely physical perspective, A_G, A_E, and T are related by the power law $T^{1/2}A_G = kA_E^{5/4}$. (The exponent 5/4 is the only value for which the constant k is adimensional.)

We first tested whether our model based on the minimization of the effective free energy of a self-avoiding surface could explain the well-known fractal folding of a self-avoiding surface: paper. We examined how the exposed surface area of crumpled paper balls, A_E, scales with increasing total surface area, A_T, and thickness, T, of office paper (in this case, under forces applied externally by the experimenter's hands). As shown in **Fig. 2A**, $A_T \approx A_E^{1.234\pm0.033}$ for crumpled single sheets, a value similar to that for gyrencephalic cortices. Increasing T (by stacking sheets before crumpling) displaces the curves to the right (**Fig. 2A**) but leaves their slope largely unaltered, resulting in similar-looking but less folded paper balls (**Fig. 2B**). However, the product $T^{1/2}A_T$ varies proportionately to $A_E^{1.105\pm0.022}$ as a single, universal power function across all paper balls of different surface

areas and thicknesses (Fig. 2C), as predicted by our model. This conformity indicates that the coarse-grained folding of a sheet of paper subjected to external compression depends simply on a combination of its surface area and thickness.

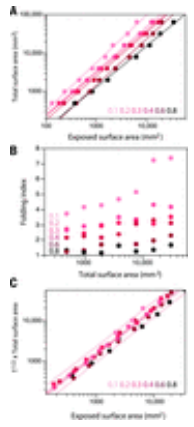

View larger version:

In this page In a new window

Download PowerPoint Slide for Teaching

Fig. 2. The degree of folding of crumpled paper balls is a function of surface area and thickness as predicted by our model.

(**A**) Relationship between total surface area of A4 to A11 sheets of office paper and the exposed surface area of the crumpled sheet of paper, with a power function of exponent 1.234 ± 0.033 for a single sheet of thickness 0.1 mm. (**B**) Increasing the thickness of the paper to be crumpled by stacking two to eight sheets displaces the curves to the right, that is, decreases the folding index of the resulting paper balls. (**C**) However, all crumpled paper balls of varying total surface area and thickness exhibit the same relationship, with the product $T^{1/2}A_T$ varying proportionately to $A_E^{1.105\pm0.022}$ ($r^2 = 0.983$, $P < 0.0001$). Color gradations correspond to thickness in millimeters, as shown in each panel.

We next examined whether our model predicts the folding of the mammalian cerebral cortex by plotting the product $T^{1/2}A_G$ as a function of A_E for the combined data sets. This yielded a power function with an exponent of 1.329 ± 0.014, with a very high r^2 of 0.996 for the noncetacean gyrencephalic species in the combined data sets (Fig. 3A, red line). Note that this function, although calculated for gyrencephalic species, overlaps with lissencephalic species. Including lissencephalic species (but still excluding cetaceans) actually improved the fit, with $r^2 = 0.998$, and yielded an exponent of 1.305 ± 0.010, which is close to the expected value of 1.25. Adding cetaceans to the analysis resulted in a small change of the fit (Fig. 3A, black line). Remarkably, the function fitted exclusively for lissencephalic species also predicted the relationship between $T^{1/2}A_G$ and A_E in gyrencephalic species (Fig. 3A, green line)—and species such as the manatee and other afrotherians are no longer outliers.

Fig. 3. The degree of folding of the mammalian cerebral cortex is a single function of surface area and thickness across lissencephalic and gyrencephalic species alike, although thickness scales as order-specific functions of cortical surface area.

(**A**) The product $T^{1/2}A_G$ varies with $A_E^{1.329\pm0.014}$ ($r^2 = 0.996$, $P < 0.0001$) across noncetacean gyrencephalic

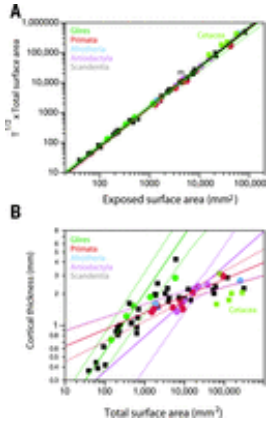

View larger version:

In this page In a new window

Download PowerPoint Slide for Teaching

species in the combined data set (red line), with $A_E^{1.325\pm0.009}$ (r^2 = 0.997, P < 0.0001, k = 0.157 ± 0.012) across all species (including cetaceans; black line), and with $A_E^{1.292\pm0.027}$ (r^2 = 0.994, P < 0.0001) across lissencephalic species alone (green line). Note that the function plotted for lissencephalic species predicts the product $T^{1/2}A_G$ for gyrencephalic species equally well as the functions plotted for gyrencephalic species themselves. (**B**) Cortical thickness varies with cortical surface area $A_G^{0.555\pm0.053}$ (r^2 = 0.887, P < 0.0001) across lissencephalic species in the combined data set (green line), but with $A_G^{0.160\pm0.025}$ (r^2 = 0.703, P < 0.0001) across primates (red line), and with $A_G^{0.334\pm0.072}$ (r^2 = 0.879, P = 0.0185) across artiodactyl species (pink line). All fits exclude cetaceans. Dashed lines indicate the 95% confidence intervals for the fitted functions.

Given the theoretical relation $T^{1/2}A_G = kA_E^{1.25}$, it follows that lissencephalic species (for which $A_G = A_E$) are those that meet the condition $T = k^2A_G^{1/2}$. In contrast, all species for which $T < k^2A_G^{1/2}$ are predicted to be gyrencephalic, with $A_G > A_E$ (the alternative where $T > k^2A_G^{1/2}$ would result in $A_G < A_E$, which is geometrically impossible). Indeed, in the combined data set, we find that $T \approx A_G^{0.555\pm0.053}$ (P < 0.0001) across lissencephalic species (**Fig. 3B**, green line). All gyrencephalic species data points fall to the right of the lissencephalic distribution; that is, their A_G values are larger than predicted for a cortical thickness that would allow lissencephaly. The precise relationship between T and A_G across gyrencephalic species differs across orders, with a much smaller exponent for primates than for artiodactyls (**Fig. 3B**, red and pink lines). Thus, within the single universal relationship that describes cortical expansion, there is a transition point between smooth and folded cortices: Gyrencephaly ensues when A_G expands in area faster than T^2. For gyrencephalic species, the rate of expansion of cortical thickness relative to expansion of the cortical surface varies across orders, but the product $T^{1/2}A_G$ still varies as a universal function of $A_E^{1.26}$ to $A_E^{1.33}$.

We also found the same universality between the product $T^{1/2}A_G$ and A_E across coronal sections along the anteroposterior axis of the cortical hemisphere of a single individual, of different individuals, and even different species ranging from small rodents to human and elephant (fig. S1).

The finding that A_E scales across all lissencephalic and gyrencephalic mammals (and even across species usually regarded as outliers such as the manatee and cetaceans) as a single power law of $T^{1/2}A_G$ indicates that gyrification is an intrinsic property of any mammalian cortex. Further, because the degree of folding can be

described by the simple equation generated by our model (which also applies to crumpled sheets of paper), folding must occur as it minimizes the effective free energy of the cortical surface. Folding is therefore an intrinsic, fractal property of a self-avoiding surface, whether biological or not, subjected to crumpling forces. As such, this scaling of cortical folding does not depend on numbers of neurons or how they are distributed in the cortical sheet, but simply on the relative lateral expansion of this sheet relative to its thickness, regardless of how densely neurons are distributed within it.

The finding that cortical folding scales universally across clades, species, individuals, and parts of the same cortex implies that the single mechanism based on the physics of minimization of effective free energy of a growing surface subject to inhomogeneous bulk stresses applies across cortical development and evolution. This is in stark contrast to previous conclusions that different mechanisms regulated folding at different levels (*7*); such conclusions may reflect the traditional emphasis on the relationship between folding degree and brain volume (*1*, *8*), which is indeed diverse across orders, across species, and across individuals of a same species (*6*, *8*). Also, the dependence of cortical folding on a simple combination of A_G and T implies that any alterations, such as defects in cell migration, that lead to increased T or decreased A_G (or both) are expected to decrease cortical folding, exactly as found in human pathological lissencephaly (*28*). This might also be the case for the lissencephalic brain of birds, where a very thick telencephalon of small surface area surrounds the subpallial structures.

Finally, our findings indicate that cortical folding did not evolve, in the sense of a new property specific to some clades but not others. Similarly, there is no such thing as “secondary lissencephaly” (*29*), nor are there two clusters of gyrencephaly (*9*). Rather, what has evolved, we propose, is a faster increase in A_G relative to T^2 in development —and at different rates in different mammalian clades, which thus become gyrencephalic at different functions of A_G or different numbers of neurons.

Remarkably, there is no a priori reason for lissencephaly, considering that A_G and T ultimately result from different biological processes: lateral expansion of the progenitor cell population for A_G, radial neurogenesis and cell growth for T (*30*). Similarly, there is no a priori reason for the cortex to become gyrencephalic once past a certain surface area—unless the rate of (lateral) progenitor cell expansion inevitably outpaces the rate of (radial) neurogenesis at this point, which apparently occurs typically when A_G reaches 400 mm^2. We propose that, starting from the earliest and smallest (and smooth) mammalian brains (*31*), the cortical surface initially scaled isometrically, with $A_G \approx T^2$. Gyrencephaly ensued in each clade as soon as this lockstep growth changed, with A_G now increasing faster than T^2. Probable mechanisms involved are those that control the rate of neurogenesis and increases in cell size relative to the rate of progenitor and intermediate progenitor cell proliferation in early cortical development. Rapid increases in numbers of intermediate progenitor cells would lead to gyrencephaly, although not through the generation of larger numbers of neurons, as previously thought (*7*, *30*, *32*), but rather through the simple lateral expansion of the resulting cortical surface area at a rate faster than the cortical thickness squared.

Supplementary Materials

www.sciencemag.org/content/349/6243/74/suppl/DC1

Materials and Methods

Table S1

References (*33*–*38*)

Received for publication 13 February 2015.

Accepted for publication 11 May 2015.

References and Notes

1. M. A. Hofman, Size and shape of the cerebral cortex in mammals. I. The cortical surface. *Brain Behav. Evol.* **27**, 28–40 (1985). CrossRef Medline Web of Science Google Scholar
2. A. J. Rockel, R. W. Hiorns, T. P. Powell, The basic uniformity in structure of the neocortex. *Brain* **103**, 221–244 (1980). FREE Full Text
3. P. Rakic, A small step for the cell, a giant leap for mankind: A hypothesis of neocortical expansion during evolution. *Trends Neurosci.* **18**, 383–388 (1995). CrossRef Medline Web of Science Google Scholar
4. R. Toro, Y. Burnod, A morphogenetic model for the development of cortical convolutions. *Cereb. Cortex* **15**, 1900–1913 (2005). Abstract/FREE Full Text
5. T. Tallinen, J. Y. Chung, J. S. Biggins, L. Mahadevan, Gyrification from constrained cortical expansion. *Proc. Natl. Acad. Sci. U.S.A.* **111**, 12667–12672 (2014). Abstract/FREE Full Text
6. K. Zilles, N. Palomero-Gallagher, K. Amunts, Development of cortical folding during evolution and ontogeny. *Trends Neurosci.* **36**, 275–284 (2013). CrossRef Medline Web of Science Google Scholar
7. E. Lewitus, J. Kelava, W. B. Huttner, Conical expansion of the outer subventricular zone and the role of neocortical folding in evolution and development. *Front. Hum. Neurosci.* **7**, 424 (2013). CrossRef Medline Google Scholar
8. P. Pillay, P. R. Manger, Order-specific quantitative patterns of cortical gyrification. *Eur. J. Neurosci.* **25**, 2705–2712 (2007). CrossRef Medline Web of Science Google Scholar
9. E. Lewitus, J. Kelava, A. T. Kalinka, P. Tomancak, W. B. Huttner, An adaptive threshold in mammalian neocortical evolution. *PLOS Biol.* **12**, e1002000 (2014). CrossRef Medline Google Scholar
10. F. A. C. Azevedo, L. R. B. Carvalho, L. T. Grinberg, J. M. Farfel, R. E. L. Ferretti, R. E. P. Leite, W. J. Filho, R. Lent, S. Herculano-Houzel, Equal numbers of neuronal and nonneuronal cells make the

human brain an isometrically scaled-up primate brain. *J. Comp. Neurol.* **513**, 532–541 (2009). CrossRef Medline Web of Science Google Scholar

11. M. Gabi, C. E. Collins, P. Wong, L. B. Torres, J. H. Kaas, S. Herculano-Houzel, Cellular scaling rules for the brains of an extended number of primate species. *Brain Behav. Evol.* **76**, 32–44 (2010). CrossRef Medline Web of Science Google Scholar

12. S. Herculano-Houzel, B. Mota, R. Lent, Cellular scaling rules for rodent brains. *Proc. Natl. Acad. Sci. U.S.A.* **103**, 12138–12143 (2006). Abstract/FREE Full Text

13. S. Herculano-Houzel, C. E. Collins, P. Wong, J. H. Kaas, Cellular scaling rules for primate brains. *Proc. Natl. Acad. Sci. U.S.A.* **104**, 3562–3567 (2007). Abstract/FREE Full Text

14. S. Herculano-Houzel, P. Ribeiro, L. Campos, A. Valotta da Silva, L. B. Torres, K. C. Catania, J. H. Kaas, Updated neuronal scaling rules for the brains of Glires (rodents/lagomorphs). *Brain Behav. Evol.* **78**, 302–314 (2011). CrossRef Medline Web of Science Google Scholar

15. S. Herculano-Houzel, K. Avelino-de-Souza, K. Neves, J. Porfírio, D. Messeder, L. Mattos Feijó, J. Maldonado, P. R. Manger, The elephant brain in numbers. *Front. Neuroanat.* **8**, 46 (2014). CrossRef Medline Google Scholar

16. R. S. Kazu, J. Maldonado, B. Mota, P. R. Manger, S. Herculano-Houzel, Cellular scaling rules for the brain of Artiodactyla include a highly folded cortex with few neurons. *Front. Neuroanat.* **8**, 128 (2014). CrossRef Medline Google Scholar

17. K. Neves. F. M. Ferreira, F. Tovar-Moll, N. Gravett, N. C. Bennett, C. Kaswera, E. Gilissen, P. R. Manger, S. Herculano-Houzel, Cellular scaling rules for the brain of afrotherians. *Front. Neuroanat.* **8**, 5 (2014). CrossRef Medline Google Scholar

18. D. K. Sarko, K. C. Catania, D. B. Leitch, J. H. Kaas, S. Herculano-Houzel, Cellular scaling rules of insectivore brains. *Front. Neuroanat.* **3**, 8 (2009). CrossRef Medline Google Scholar

19. S. Herculano-Houzel, B. Mota, P. Wong, J. H. Kaas, Connectivity-driven white matter scaling and folding in primate cerebral cortex. *Proc. Natl. Acad. Sci. U.S.A.* **107**, 19008–19013 (2010). Abstract/FREE Full Text

20. L. Ventura-Antunes, B. Mota, S. Herculano-Houzel, Different scaling of white matter volume, cortical connectivity, and gyrification across rodent and primate brains. *Front. Neuroanat.* **7**, 3 (2013). CrossRef Medline Google Scholar

21. P. F. M. Ribeiro, L. Ventura-Antunes, M. Gabi, B. Mota, L. T. Grinberg, J. M. Farfel, R. E. Ferretti-Rebustini, R. E. Leite, W. J. Filho, S. Herculano-Houzel, The human cerebral cortex is neither one nor many: Neuronal distribution reveals two quantitatively different zones in the gray matter, three in the white matter, and explains local variations in cortical folding. *Front. Neuroanat.* **7**, 28 (2013). CrossRef Medline Google Scholar

22. H. Elias, D. Schwartz, Cerebro-cortical surface areas, volumes, lengths of gyri and their interdependence in mammals, including man. *Z. Saugetierkd.* **36**, 147–163 (1971). Google Scholar

23. R. L. Reep, T. J. O'Shea, Regional brain morphometry and lissencephaly in the Sirenia. *Brain Behav. Evol.* **35**, 185–194 (1990). CrossRef Medline Web of Science Google Scholar

24. T. M. Mayhew, G. L. Mwamengele, V. Dantzer, S. Williams, The gyrification of mammalian cerebral cortex: Quantitative evidence of anisomorphic surface expansion during phylogenetic and ontogenetic development. *J. Anat.* **188**, 53–58 (1996). Medline Web of Science Google Scholar

25. Y. Kantor, M. Kardar, D. R. Nelson, Tethered surfaces: Statics and dynamics. *Phys. Rev. A* **35**, 3056–3071 (1987). CrossRef Medline Google Scholar

26. D. H. Smith, Stretch growth of integrated axon tracts: Extremes and exploitations. *Prog. Neurobiol.* **89**, 231–239 (2009). CrossRef Medline Web of Science Google Scholar

27. D. H. Smith, J. A. Wolf, D. F. Meaney, A new strategy to produce sustained growth of central nervous system axons: Continuous mechanical tension. *Tissue Eng.* **7**, 131–139 (2001). CrossRef Medline Web of Science Google Scholar

28. S. E. Hong, Y. Y. Shugart, D. T. Huang, S. A. Shahwan, P. E. Grant, J. O. Hourihane, N. D. Martin, C. A. Walsh, Autosomal recessive lissencephaly with cerebellar hypoplasia is associated with human *RELN* mutations. *Nat. Genet.* **26**, 93–96 (2000). CrossRef Medline Web of Science Google Scholar

29. I. Kelava, F. Lewitus, W. B. Huttner, The secondary loss of gyrencephaly as an example of evolutionary phenotypical reversal. *Front. Neuroanat.* **7**, 16 (2013). CrossRef Medline Google Scholar

30. J. H. Lui, D. V. Hansen, A. R. Kriegstein, Development and evolution of the human neocortex. *Cell* **146**, 18–36 (2011). CrossRef Medline Web of Science Google Scholar

31. T. B. Rowe, T. E. Macrini, Z. X. Luo, Fossil evidence on origin of the mammalian brain. *Science* **332**, 955–957 (2011). Abstract/FREE Full Text

32. I. Reillo, C. de Juan Romero, M. A. García-Cabezas, V. Borrell, A role for intermediate radial glia in the tangential expansion of the mammalian cerebral cortex. *Cereb. Cortex* **21**, 1674–1694 (2011). Abstract/FREE Full Text

33. S. Herculano-Houzel, R. Lent, Isotropic fractionator: A simple, rapid method for the quantification of total cell and neuron numbers in the brain. *J. Neurosci.* **25**, 2518–2521 (2005). Abstract/FREE Full Text

34. S. Herculano-Houzel, C. S. von Bartheld, D. J. Miller, J. H. Kaas, How to count cells: The advantages and disadvantages of the isotropic fractionator compared with stereology. *Cell Tissue Res.* **360**, 29–42 (2015). CrossRef Medline Google Scholar

35. D. C. Van Essen, A tension-based theory of morphogenesis and compact wiring in the central nervous system. *Nature* **385**, 313–318 (1997). CrossRef Medline Web of Science Google Scholar

36. P. V. Bayly, R. J. Okamoto, G. Xu, Y. Shi, L. A. Taber, A cortical folding model incorporating stress-

dependent growth explains gyral wavelengths and stress patterns in the developing brain. *Phys. Biol.* **10**, 016005 (2013). CrossRef Medline Google Scholar

37. D. Nelson, T. Piran, S. Weinberg, *Statistical Mechanics of Membranes and Surfaces* (World Scientific, Singapore, 1989).

38. V. J. Wedeen, D. L. Rosene, R. Wang, G. Dai, F. Mortazavi, P. Hagmann, J. H. Kaas, W. Y. Tseng, The geometric structure of the brain fiber pathways. *Science* **335**, 1628–1634 (2012). Abstract/FREE Full Text

39. **Acknowledgments:** Supported by Conselho Nacional de Desenvolvimento Científico e Tecnológico, Fundação de Amparo à Pesquisa do Estado do Rio de Janeiro, INCT/MCT, and the James S. McDonnell Foundation. Data reported in the paper are presented in the supplementary materials.

The editors suggest the following Related Resources on *Science* sites

In *Science* Magazine

PERSPECTIVE
BRAIN EVOLUTION
Knowing when to fold them
Georg F. Striedter and Shyam Srinivasan
Science 3 July 2015: 31-32.
Summary **Full Text** **Full Text (PDF)**

Leave a comment (0)